



INFN/TC-02/15  
**5 Giugno 2002**

**THE DESCRIPTION OF THE TEMPHURA-METER**

M. Anghinolfi<sup>1</sup>, M. Battaglieri<sup>1</sup>, P. Cocconi<sup>1</sup>, R. De Vita<sup>1</sup>, F. Parodi<sup>1</sup>,  
M. Ripani<sup>1</sup>, A. Rottura<sup>1</sup>, M. Taiuti<sup>2</sup>, S. Zavatarelli<sup>2</sup>

<sup>1</sup>) *INFN, Sezione di Genova, Via Dodecaneso 33, I-16146 Genova, Italy* <sup>2</sup>) *Dipartimento di Fisica dell'Università di Genova, Via Dodecaneso 33, I-16146 Genova, Italy*

**Abstract**

We built an apparatus (TempHuRA-meter) to measure the relevant physical quantities (TEMPerature, HUmidity, Rotation and Acceleration) during the deployment tests of the ANTARES sector line. A brief description of the TempHuRA components, its mechanical and electrical lay-out as well as the calibration procedures are reported. The measurements taken during the December 2001 deployment test are discussed.

PACS.: 95.55.Vj

## 1 Introduction

The role of neutrinos in the study of galactic and extra-galactic phenomena is well known [1]. The small cross-section permits the  $\nu$  to travel for long distances in the Universe and their detection would allow the investigation of processes otherwise screened by the matter. The detection of high energy neutrinos requires a large amount of matter to convert it into a charged muon and to reconstruct the muon track. Large volumes of water (or alternatively ice) located at large depth could become very efficient detectors: a) they are located close to the Earth mantle where the neutrinos coming from the opposite hemisphere interact and are converted into a charged muon; b) the column of water located on top of them shields the atmospheric background; c) they are excellent sources of Cherenkov light for high momentum muons. Several projects in the detection of high energy neutrinos are in progress: BAIKAL[2] in the Baikal lake and AMANDA[3] in Antartides are in the process of data taking, while others as ANTARES[4], NESTOR[5], and NEMO[6] in Mediterranean Sea are in the early stage of the installation.

Under-see high energy neutrinos telescopes are in principle simple detectors involving well known technologies used in high-energy-physics laboratories (phototubes, fast electronics, trigger processing etc). However they have to be placed and work in an adverse environment: deep sea water, high pressure (up to 300 bars), difficulties in accessing and maintaining the detector components for long term operation. For these reasons, even a simple operation as the deployment of the detector has to be prepared in details, tested, and the relevant physical quantities (mechanical accelerations, string rotation, temperature and humidity inside the sealed instrumentation containers) have to be measured in order to understand the behavior of the mechanical structures and to optimize the design. TempHuRA is a compact, water-tight, pressure-resistant, stand-alone instrument able to measure the triaxial acceleration, the three components of the Earth magnetic field, the tilt angles in respect to the horizontal plane, the relative humidity and the temperature. All the analog signals are converted to digital data and recorded on a hard-disk, for the off-line analysis. A Pentium-based CPU guarantees complete flexibility in the DAQ software, while long life-time alkaline cells allows hours of continuous operation.

Following a brief description of the ANTARES line (Section 2), the single components of the TempHuRA detector will be presented in details as well as the mechanical and electrical scheme of the whole apparatus (Section 3). A short description of the data acquisition software will be given in Section 4 while the main calibrations procedures will be described in Section 5. The analysis of data collected during the December 2001 deployment test will be presented and discussed in the Section 6.

## 2 The ANTARES detector line

The ANTARES telescope aims at high energy neutrino detection by measuring the muon Cherenkov light with photomultipliers arranged as a three dimensional array in the sea at a depth of 2400 m. The detector has an effective area of 0.1 km<sup>2</sup> and consists of 10 lines (or strings) holding the PMTs. Starting from the shore, a 40 km undersea cable is used to power the system and collect signals in optical fibers. The cable enters in a junction box (JB), which converts the AC voltage and distributes the power to each detector line. The JB, connected to each line by electro-optical cables, is positioned inside a frame used for deployment and recovery operations. Each detector string is anchored on the sea bottom and maintained vertical by its buoyancy. The components of the line are the following: an anchor made of a dead weight and a recoverable structure (bottom string socket BSS), 30 elementary storeis, each with an optical module frame (OMF) supporting three optical modules (OM) and a local control module (LCM). The OMF are connected with each other by a 10 m electro-mechanical cable (EM) for a total string length of about 400 m. Each optical module is oriented at 45 degrees with respect to the equator plane to have high efficiency for tracks coming from sea bottom and minimize effects due to biofouling.

To test the line-deployment procedure, the ANTARES Collaboration built a sector line made by: 5 OMF connected to the BSS by a 100 m EM cable, and a top buoy (see fig. 1). The top OMF as well as the BSS were equipped with the TempHuRA meter described in this paper. A current-meter (velocity and direction) able to measure water pressure, salinity, and sound velocity was installed in the bottom OMF. In addition, another accelerometer provided by IFREMER with limited battery life-time, was placed on the BSS. The sector line was deployed in the ANTARES site in December 2001. The sea operations were performed with a dedicated ship (Castor): the line was deployed at a specified position, released by acoustic devices, and finally recovered at the sea surface. The test demonstrated that the ship was adequate and the deployment and recovery procedures were effective. The data recorded by the instruments located on the line were very useful for the understanding of the operations.

## 3 The TempHuRA-meter

Fig. 2 shows a picture of the TempHuRA meter. The system includes:

- a triaxial accelerometer;
- a tiltmeter and compass;

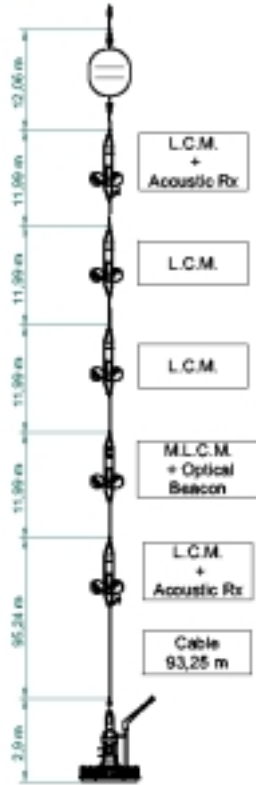


Figure 1: The ANTARES sector line: the TempHuRA meters were installed in the top LCM and on the BSS.



Figure 2: Picture of the TempHuRA-meter.

- a temperature and humidity sensor;
- an acquisition and data storage device;
- a battery package.

These elements are mounted on a holding structure made of brass rods and aluminum plates shown in fig. 3. The structure occupies the whole volume of the titanium LCM cylinder being attached to the LCM bottom flange.

### 3.1 The accelerometer

The accelerometer mounted on the TempHuRA-meter is the model 2422-010 by the Silicon Designs Inc. It is a low power consumption triaxial accelerometer module combining three orthogonally single-axis meters. Each of them contains a miniature, hermetically-sealed capacitive sense element and a dedicated amplifier. The module produces three differential analog output voltages which vary linearly with acceleration (from -4V to 4V). The 2422-010 model has an input range from -10  $g$  to 10  $g$  and a frequency response 0-600  $Hz$ . The cross axis sensitivity and the bias calibration error are both of the order

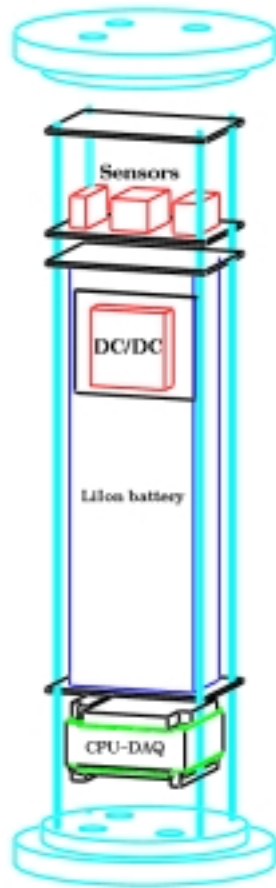


Figure 3: Schematic view of the TempHuRA-meter.

of  $\pm 0.1-0.2$  g. The required power supply is  $5V \pm 5\%$  DC with a power consumption of 100 mW.

### 3.2 The tiltmeter and compass

The tiltmeter-compass we used is the same chosen to instrument the ANTARES line [7]. The TCM2-50 by the Navigation Precision Inc. is a commercial device mounting on the same board:

- a biaxial tiltmeter;
- a triaxial magneto-meter;
- an ADC;
- a micro-controller for the 'hard-iron' calibration and the serial link communication;
- a DC/DC converter delivering a regulated voltage to the sensor.

It is able to measure the two components of the tilt angle (*pitch* and *roll* angles) respect to the horizontal (in degrees), the three components of the magnetic field (in microtesla) and the sensor board heading with respect to Magnetic North (in degrees). The board is also equipped with a thermometer giving the temperature in Celsius degrees. It requires an unregulated 12 V DC having a maximum current consumption of 20 mA. The communication is assured by an RS 232 serial link.

### 3.3 The temperature and humidity meter

The humidity sensor is the HIH-3605-A-CP single-chip by the Honeywell Inc. using an industrially proven thermoset polymer, three layer capacitance construction, and on-chip silicon integrated output signal conditioning. The output of this device is a function of voltage supply, temperature and relative humidity (%RH). The V supply (around 5V DC) was continuously measured while the temperature was measured by a platinum thermoresistance Pt100 placed close to the humidity sensor's active area. The tolerance of the humidity sensor is  $\pm 2\%$  while the precision of the thermometer is about  $0.5$  °C.

### 3.4 The controller

The signals coming from the different sensors are collected and processed by a micro computer by Real Time Devices Inc., consisting of three boards: a CPU, a DAQ, and a high capacity hard disk. The CPU module (model CMM7686GX233) is based on a Cyrix MediaGXm MMX 233 MHz microprocessor with 128 Mb of SDRAM and provides standard SVGA support for an external monitor, keyboard connectors and two RS-232 serial ports. The DAQ board (model PCI4520/DM7520), connected to the motherboard through the PCI Bus, is equipped with a fully programmable 16 channels, 12 bit, 1.25 Msample/s

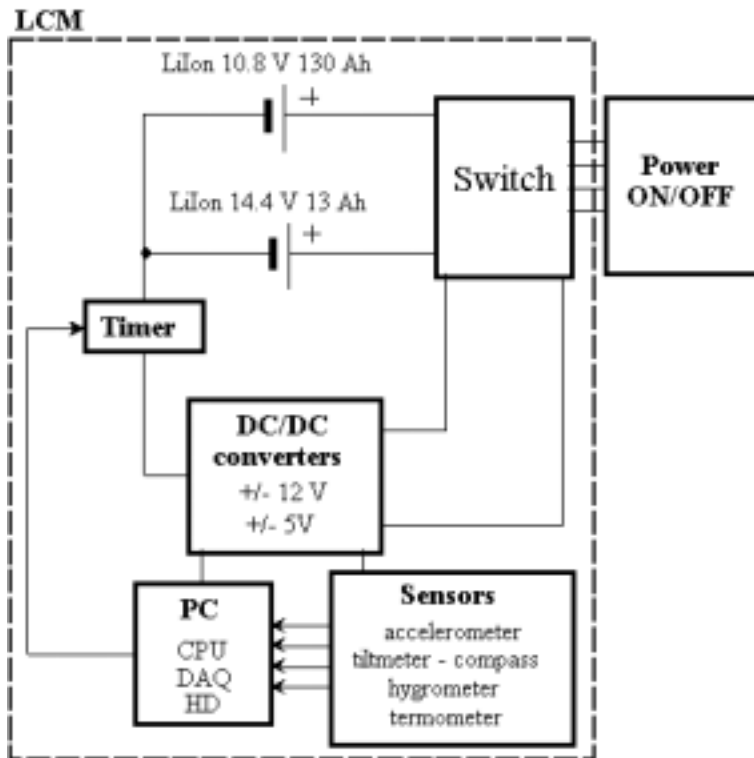


Figure 4: Electrical scheme of the TempHuRA meter.

analog-to-digital converter. The 1024 sample A/D buffer allows gap-free full speed sampling under DOS. We did not use the digital-to-analog converter and the timer/counters also present on the board. The data were stored on a high speed 5Gb hard disk connected to the same PCI bus.

### 3.5 Electrical lay-out

Fig. 4 shows a schematic diagram of the electric connections. The power is provided by two sets of Lithium-Ion batteries providing a total autonomy of about 80 hours. Two DC/DC converters transform the 10.8 V and 14.4 V battery output into  $\pm 12\text{ V}$  (TCM2 and DAQ module) and  $\pm 5\text{ V}$  (CPU, accelerometer, hygrometer, and PT100). An external removable circuit connected through a water-tight penetrator is used to switch on/off the TempHuRA. A watch-dog system was realized by inserting a timer which resets the power supply line of the whole apparatus unless an acknowledge signal is received from the CPU.



#### 4 The Data Acquisition software

The data acquisition is driven by a C-based code running under ROMDOS on the micro computer. The connection between the CPU module and the TCM2 is performed with a standard RS232 serial interface. The full set of data measured by the TCM2 (tilt angles, magnetic heading, magnetic field components, and temperature) is transferred to the CPU on demand, and stored in the CPU memory. The A/D conversion of the three-axial accelerometer, PT100, and humidity sensor is performed by DAQ board. The 16 input channels are configured in differential mode, providing 8 low-noise channels. Six of the eight channels are used to acquire the 5 above-mentioned quantities and to monitor the 5 V voltage supply used to power accelerometer, Pt100 and humidity sensor. The data are stored in the 8Mbit FIFO of the DAQ board and then transferred to the CPU memory on demand.

Two different sampling frequencies have been adopted for the DAQ board and the TCM2/RS232 port. Each DAQ channel is sampled at 200 Hz in continuous mode. Data stored in the DAQ FIFO are transferred to the CPU module every 2 seconds without interruptions of the acquisition process. The data are finally averaged over a period of 50 ms corresponding to 10 sample to reduce the electronic noise, obtaining an effective sampling frequency of 20 Hz. Each 2 second a reading request is also sent to the TCM2. A 0.5 Hz frequency is in fact sufficient to detect the slow variation of the tilt and heading due to the movement of the line in water, while the 20 Hz frequency chosen for the DAQ board acquisition allows the detection of the mechanical vibrations of the line. The data are initially stored in the CPU memory and then saved in text files every 30 seconds. A first file is used to store the 20 Hz data of the triaxial accelerometer. A separate file is used to store the 0.5 Hz data of the TCM2 as well as the PT100, hygrometer, accelerometer values, and a time stamp in seconds. New files are opened every 15 min. to maintain a small file size. This configuration results in a data volume of  $\sim 2.1$  MB per hour, i.e. 25 MB for a 12 hours deployment test.

The acquisition code performs systematic checks on the consistency of the data to detect possible instrument failures or connectivity problems. In case of failure, a software reset is sent to the involved system. This has been shown to be necessary for the TCM2 which has been found to give incomplete information if subjected to strong vibrations. Furthermore the timer described in Sec. 3.5 has been programmed to provide an hardware reset every 15 minutes if the CPU is not responding.

## 5 Tests and calibrations in the laboratory

Each instrument was tested before being installed in the TempHuRA:

- Tilt meter and compass  
Resolution, accuracy and reproducibility of TCM2 have been object of extensive qualification tests (for details see ref. [8]). Briefly, the tilt deviation and resolution are respectively less than  $0.3^\circ$  and  $0.1^\circ$ . The heading accuracy, after the compensation of magnetic anomalies through the ‘hard-iron’ calibration available on board, is typically  $1-2^\circ$ . However, strong magnetic interferences ( $B > 40 \mu\text{T}$ ) could seriously affect the heading accuracy. The maximum noise jitter for the 3 magnetic sensors is  $0.3 \mu\text{T}$  and the resulting heading noise jitter is  $0.6^\circ$ .
- Accelerometer  
The offset on each axis was derived measuring the gravitational acceleration and corrected in the software. The offset stability was found to be better than 1% of the full scale compatible with the instrument specifications.
- Temperature sensors  
The calibration was made by comparison with a high precision thermocouple (Fluke 52 K/J, accuracy  $0.1^\circ\text{C}$ ) in the  $0-40^\circ\text{C}$  range. The resulting accuracy was  $\pm 0.5^\circ\text{C}$
- Hygrometers Honeywell HIH-3605 has a resolution of 2% at  $25^\circ\text{C}$  and the factory calibration has been adopted.

Several tests were performed on the TempHuRA after the full assembling in the LCM to check performances.

- Heat dissipation  
The power consumption is typically 17 W. Inside the LCM the heat could be dissipated only through the container walls: a maximum temperature of  $35^\circ\text{C}$  was reached after 15 hours of continuous operation (the environmental temperature was about  $24^\circ\text{C}$ ). In these conditions the heat dissipation is enough to prevent any damage to electronics. In real operations (environmental water temperature  $\sim 13^\circ\text{C}$ ) an even lower asymptotic temperature is expected.
- TCM2 calibration in presence of magnetic interferences  
The goal of the test was to check the accuracy of the compass measurement given by the TCM2 card once located on the BSS and on the OMF. The TCM2 calibration was performed in presence of electromagnetic perturbations arising from all

the electronic devices placed inside TempHuRA and the metal frames. Obviously major perturbations are expected from the 3 tons of iron of the BSS. Details of this test can be found in [9]. Briefly, BSS (or OMF) was first positioned at a '0°' reference point and several readings were collected from the uncalibrated TCM2 card (head, Bx, By, Bz). The same measurement was then repeated in steps of 45° from the initial position. Then, the automatic 'hard-iron' calibration was performed and the resulting accuracy was checked repeating the above procedure. The automatic procedure was successful for the TempHuRA mounted in the OMF while a residual distortion was still present in the case of the BSS. To eliminate this effect, we applied manually the 'hard-iron' calibration procedure, removing completely this distortion.

- Tilt-meter and accelerometer comparisons

The pitch and roll angles measured by the TCM2 were compared with the same quantities derived from the triaxial accelerometer. A fair agreement between the two instruments was found. In particular, the accelerometer could be used to deduce the tilt for angles greater than 20° when the TCM2 saturates.

- Accelerometer test

The accelerometers response in dynamic conditions was tested in several ways, for example inducing movements up and down with a pulley or horizontally with a cart. Velocity and covered distance obtained by integrating the acceleration were verified to be correctly reconstructed. Finally the acceleration was measured during the TempHuRA transport from CPPM to La Seyne. A maximum value of 1 g with respect to gravity was registered.

Time	Deployment status
10:15	Deployment of BSS
10:24	Deployment of first OMF
10:40	Deployment of second OMF
10:45	Deployment of third OMF
10:49	Deployment of fourth OMF
10:57	Deployment of fifth OMF
11:05	Deployment of the buoy
11:11	Start descent at 0.5 m/s
12:34	Stop at 1920 m
13:45	Start descent
14:04	Stop at 2370 m, 50 m from sea bed
14:33	BSS is lowered on the sea bed and then lifted
14:40	BSS is lowered on the sea bed
14:45	BSS is lifted and left and 3 mm from sea bed
14:56	BSS is lowered on the sea bed
15:20	BSS is lifted up and then lowered on the sea bed
15:30	Release of the Deep sea cable
17:55	Release of anchor of BSS
18:15	Buoy at sea surface
18:50	Beginning of line recovery
19:50	The line is on board

Table 1: Main phases of the deployment test.

## 6 The results of the deployment test

The deployment test was performed on December 1<sup>st</sup> 2001 in the Antares Site. The line, assembled in La Seyne, was deployed at a depth of 2400 m, left free at the sea bottom, and then recovered. The full operation lasted for approximately 10 hours: a brief summary of the different steps of the deployment test is reported in table 1.

The TempHuRA mounted on the OMF was switched on before the line immersion and operated successfully for the full test. Unfortunately the TempHuRA mounted on the BSS worked only for a short time on board and no data were recorded during the deployment. The data recorded by the first module were analyzed and the results are reported below.

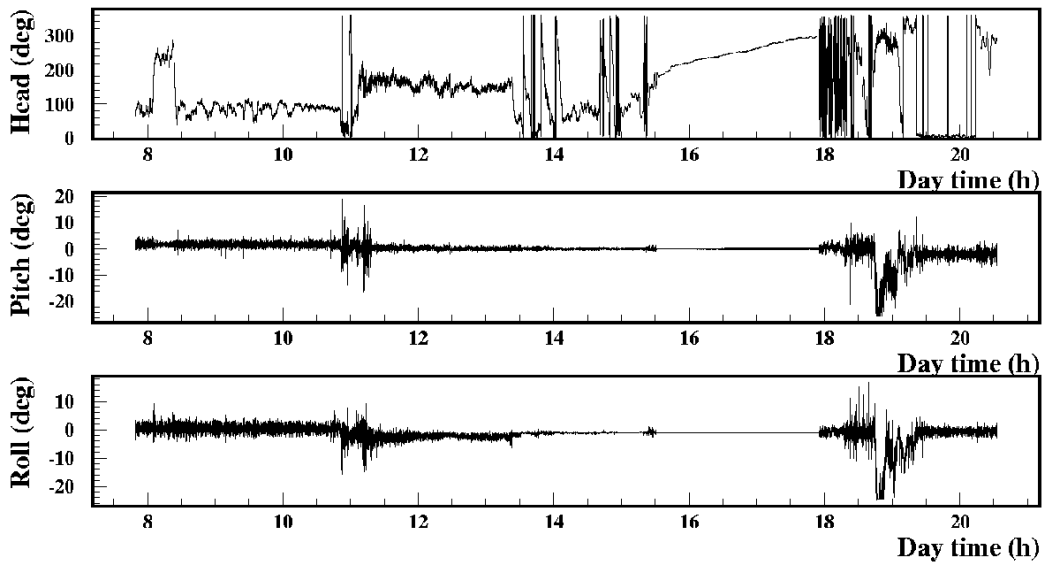


Figure 5: Head, pitch, and roll measured by TempHuRA as a function of time for the entire deployment test.

## 6.1 Temperature and humidity

The temperature measured inside the instrumented LCM module remained stable around 20°C during the whole test. The measured humidity was around 70%, stable in time after a fast rise at the switch-on of the TempHuRA. Two spikes were recorded simultaneously to the OMF deployment and recovery. Mechanical shocks could account for this behavior, even if some humidity release from the system can not be excluded.

## 6.2 Line rotation

The TCM2 data were analyzed to study the detector rotations during the different phases of the deployment. Fig. 5 shows the recorded values of head, pitch and roll as a function of day time for the full test. The measured head, limited between 0-360 deg, was transformed into the corresponding absolute quantity which accounts for the real number of turns (see fig. 6). The most significant deployment phases are blowed-up in figs. 7 and 8. The three plots in fig. 7 show respectively the beginning of the OMF descent, the behavior of the line when stopped at 500m from the sea bed, the first contact of the BSS with the sea bed and the rotation induced by lifting and lowering the line. While the line shows only small oscillations when hung to the boat, full turn rotations were determined by the change in tension of the EM cable. The two plots in fig. 8 show respectively the behavior of the

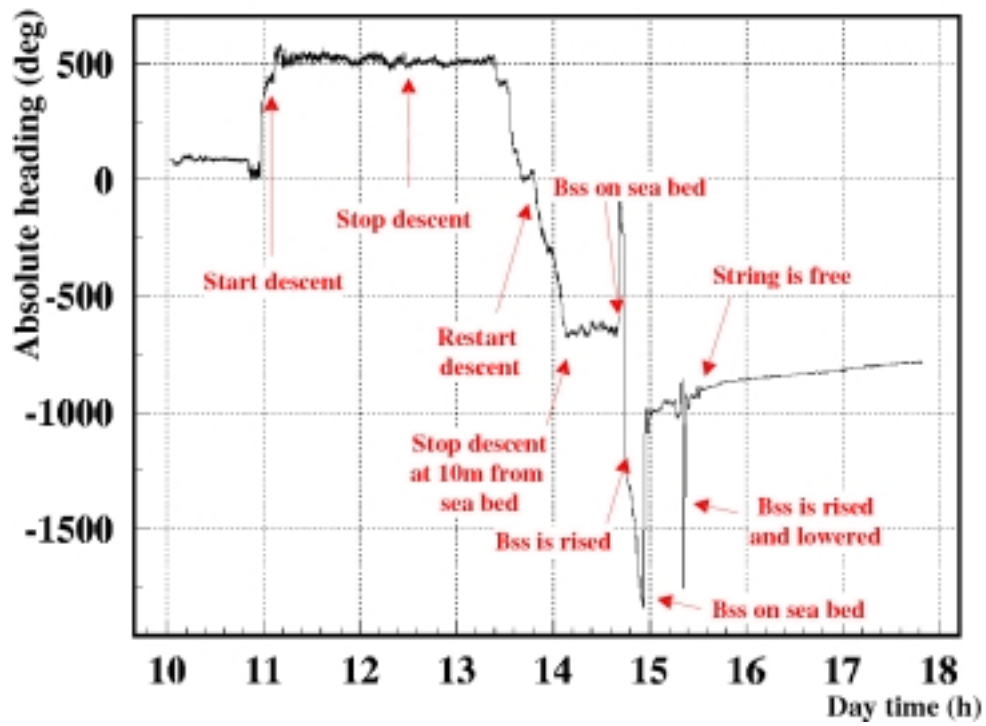


Figure 6: Absolute heading during the entire deployment test: the main steps are indicated.

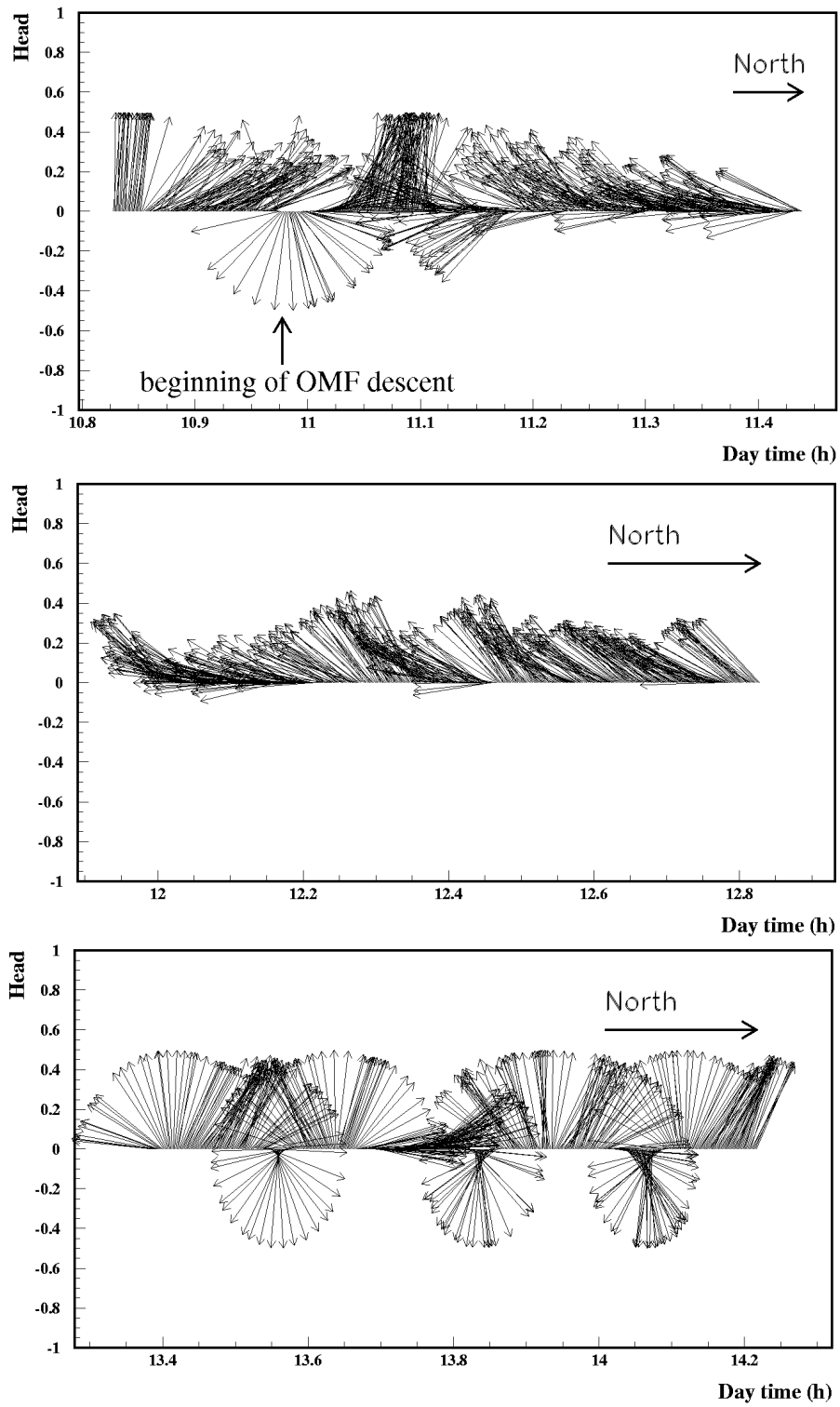


Figure 7: Top: beginning of OMF descent; middle: line oscillations at 500m from sea bed; bottom: first contact of the BSS with the sea bed.

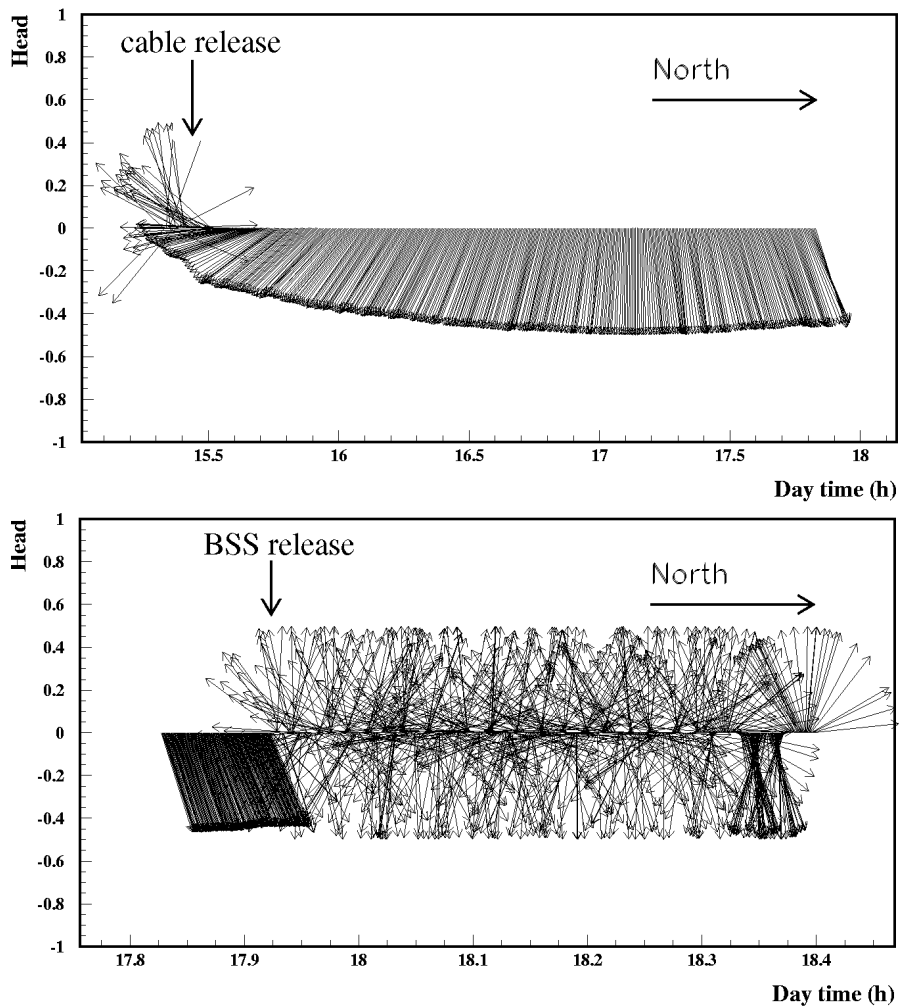


Figure 8: Top: rotation of the free line; bottom: ascent of the line after BSS release.

free line after the release of the deep-sea cable and the ascent of the line after the BSS release. Data taken immediately after the release of the anchor of the BSS were analyzed in details to extract the rotation speed of the line to understand the line behavior at the beginning of the ascent. The result is shown in fig. 9 which represent the absolute head as a function of time. The slope of the data in 140s-160s time range, gives a rotation speed of  $8 \pm 1$  deg/sec. In addition to the rotation data, the pitch and roll angles are important to detect any significant tilt of line components. As shown in fig. 5 (top OMF TempHuRA meter data) and fig. 10 (BSS IFREMER accelerometer) no significant deviations from the horizontal plane were measured.



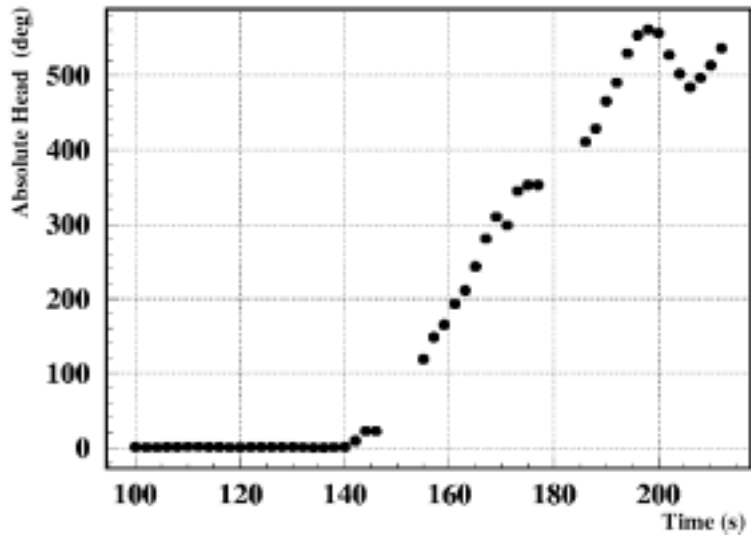


Figure 9: Absolute head immediately after the BSS anchor release.

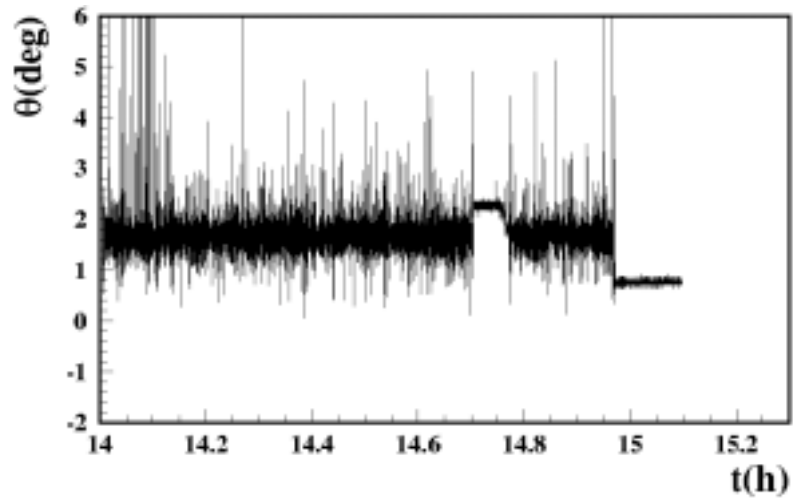


Figure 10: Angle between the z axis of the BSS IFREMER accelerometer and gravity.

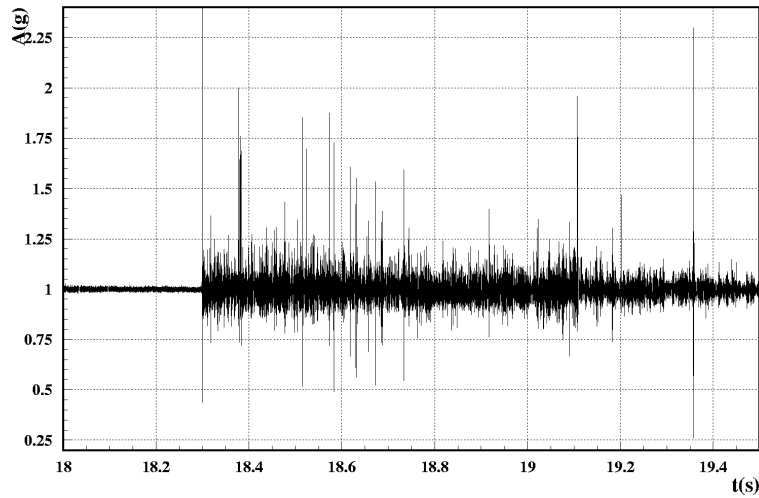


Figure 11: The maximum acceleration was recorded during line recovery.

### 6.3 Acceleration and velocity at line release and recovery

The recorded acceleration during the whole test does not show strong patterns. The maximum value was detected during the line recovery as shown in fig. 11 with a value of 2.3 g.

From the analysis of the data sampled at 20 Hz it was possible to reconstruct speed and displacement of the line in various phases of the test. As shown by the tests performed in the laboratory, the integration of the acceleration is reliable up to a time period of 20-30 seconds, while for longer intervals, the fluctuation of accelerometer offset introduce strong systematic effects. For instance, this integration was performed for data around 15:30 (see fig. 12) showing that an horizontal line displacement before the release of the deep-sea cable. This probably indicates a dragging of the line by the Castor boat when the BSS was already sitting on the sea bed. The same procedure was adopted to derive the ascent velocity of the line immediately after BSS release. Fig. 13 shows the acceleration  $z$  component during the entire ascent. The spike at 655 (minutes since 7:00) is blowed-up in fig. 14 and integrated to velocity and space. The asymptotic speed is 1.6 m/s compatible with the estimation based on recovery time [10].

### 6.4 Fourier analysis of the triaxial acceleration

To investigate the intrinsic oscillation modes of the line, we performed the Fourier analysis of the acceleration and rotation data. In particular, we studied three time intervals:

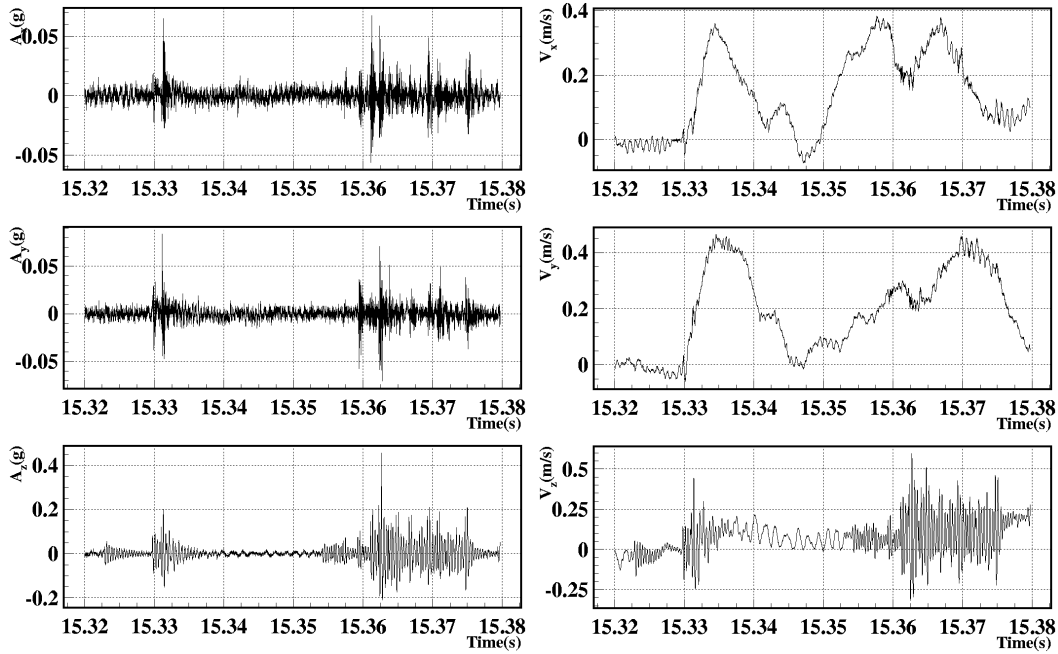


Figure 12: Left: triaxial acceleration around 15:30. The spikes observed in  $x$  and  $y$  components correspond to an horizontal displacement of the order of 10 m. Right: Reconstructed velocity.

- 8:04-8:23: acceleration measured on the boat;
- 12:57-13:27: acceleration and rotation when the line was suspended at 500 m from sea bed;
- 16:12-16:27: acceleration and rotation for free line.

The four spectra are shown in figs. 15, 16, 17 and 18, where the black line is the raw Fast Fourier Transforms (FFT) and the red line is the same quantity smoothed by a Butterworth filter. In acceleration spectra, the cut-off at 10 Hz is due to the 20 Hz sampling frequency, while in the rotation spectrum the maximum frequency is .25 Hz corresponding to 2 seconds sampling interval. The contribution of sea waves is clearly visible in the first two plots in the frequency range 0.1-0.5 Hz. In particular when the line is on the boat, this contribution is present in all three acceleration components(see fig. 15). On the contrary, when the line is suspended in water, the sea waves component is mostly visible in the vertical direction (see fig. 16). For frequency higher than 0.5 Hz, both the first and second time interval show other contributions that could be related to the boat engine. Most of these effects disappears when the line is free at the sea bottom (see fig. 17). In this case the frequency spectrum is almost flat except for a spike at 0.4 Hz

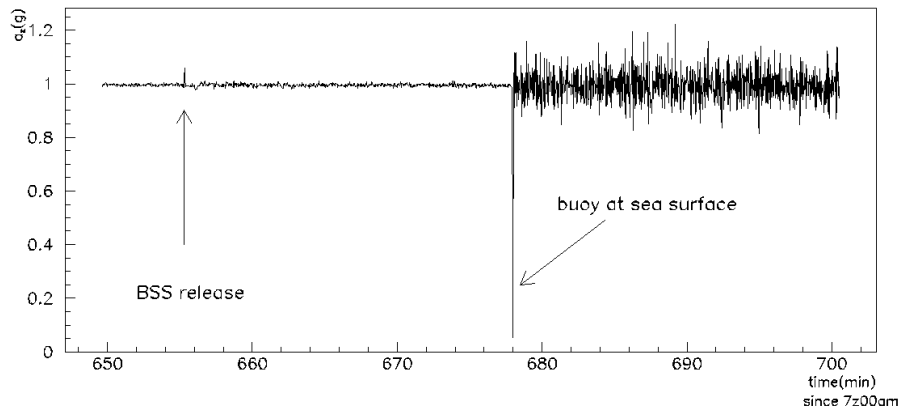


Figure 13: Acceleration  $z$  component during the line ascent.

in  $x$  and  $y$  components. Rotation spectra (see fig. 18) show also a smooth behavior in the low frequency range. The spike at  $\sim 0.07$  Hz in free line spectrum indicates a slow and weak periodic rotation of the line.

From the Fourier analysis, it is clear that the line in water is essentially stable with only weak oscillations. The main effects detected are related to the sea waves components when the line is on the boat or connected through the deep sea cable.

### 6.5 Comparative analysis of the TempHuRA data

The acceleration and the head measured by the TempHuRA meter were compared with the data recorded by the MORS VACM current meter [11] mounted on the bottom OMF and the IFREMER accelerometer [12] installed on the BSS. Fig. 19 shows the head during the entire test compared with the current direction and speed. The current direction agrees very well with the magnetic north. This can be explained considering that the direction measured by the currentmeter is relative to the magnetic north. Therefore when the current speed is low with respect to the instrumental sensitivity, this device is equivalent to a compass.

## 7 Conclusions

Operating in adverse environment conditions, new under-see neutrino telescopes require a detailed knowledge of mechanical and environmental parameters (acceleration and rotation of the detector parts, temperature and humidity inside the sealed instrumentation containers) during the critical phase of deployment.

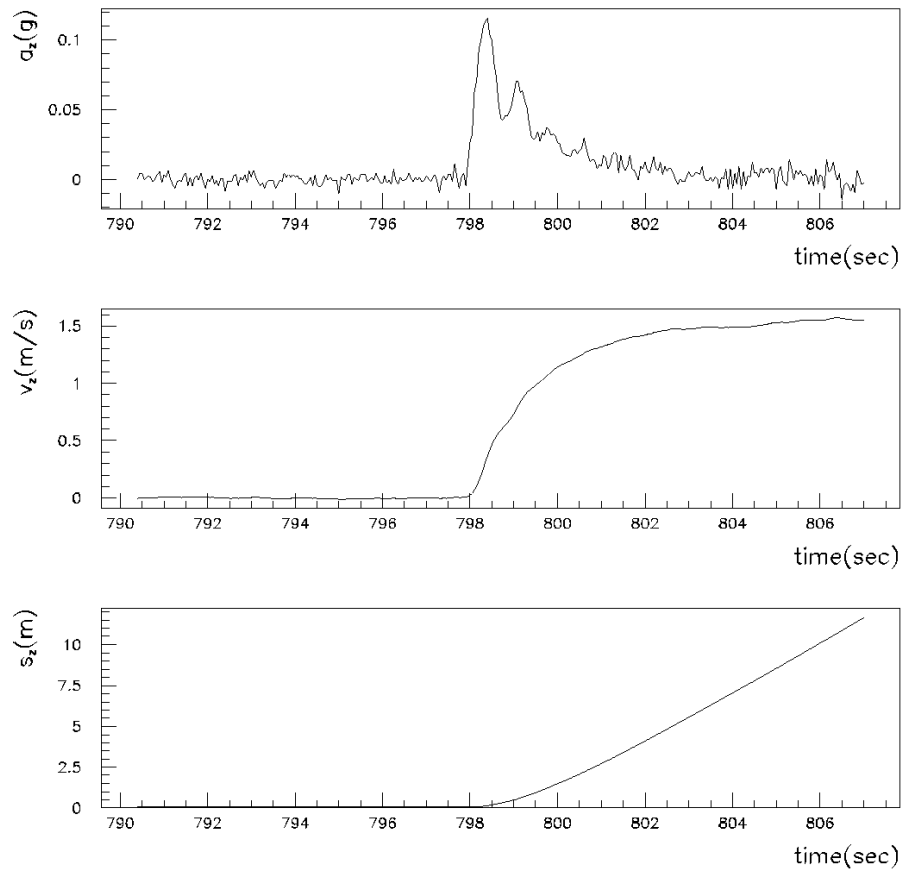


Figure 14: Acceleration and reconstructed speed and distance at the BSS release. The middle plot shows the asymptotic speed of the line is 1.6 m/s.

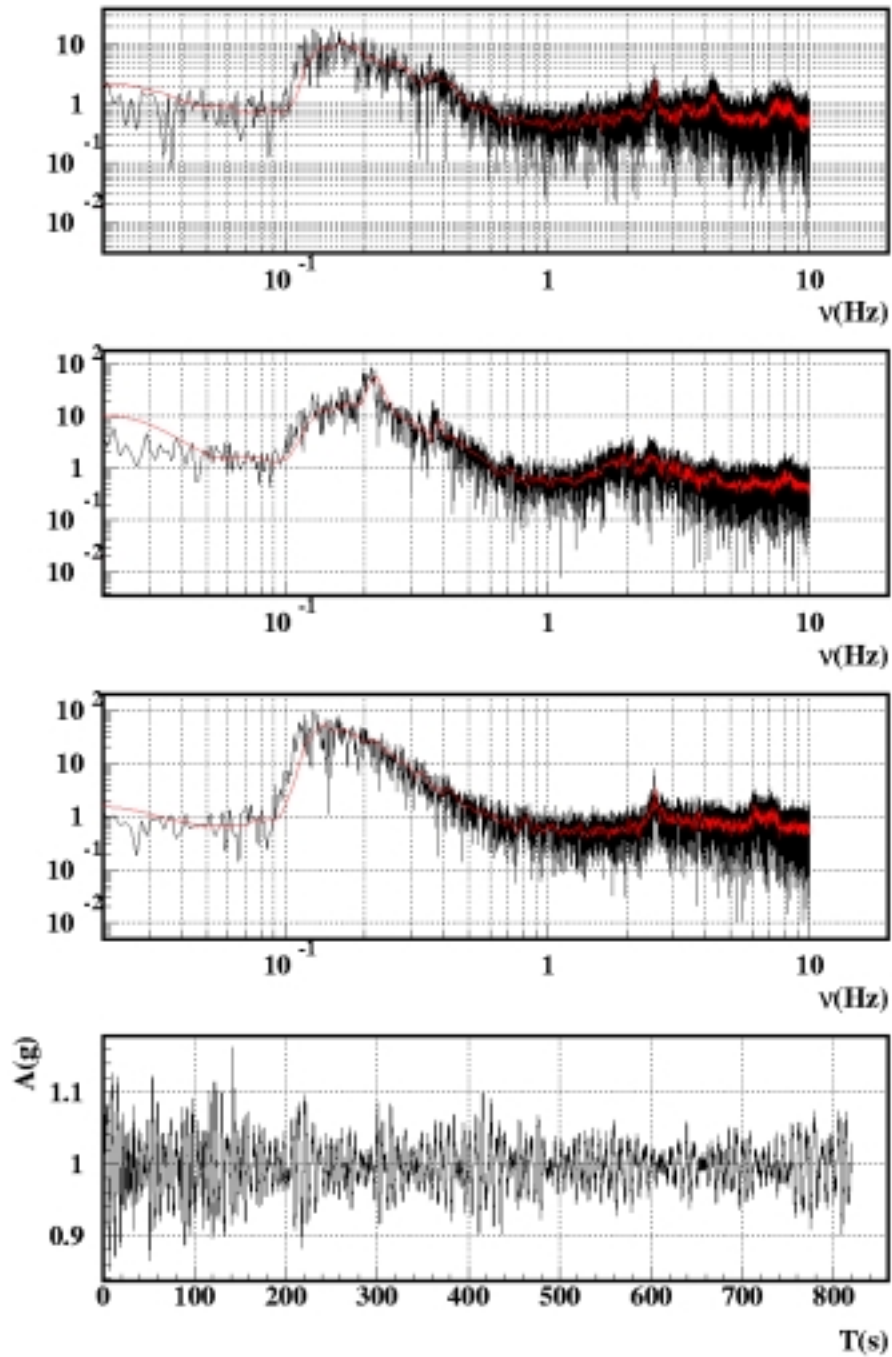


Figure 15: FFT of the acceleration measured on the boat from 8:04 to 8:23; the black line is the raw Fast Fourier Transforms and the red line is the same quantity smoothed by the Butterworth filter. Bottom plot shows the acceleration amplitude in the corresponding time interval.

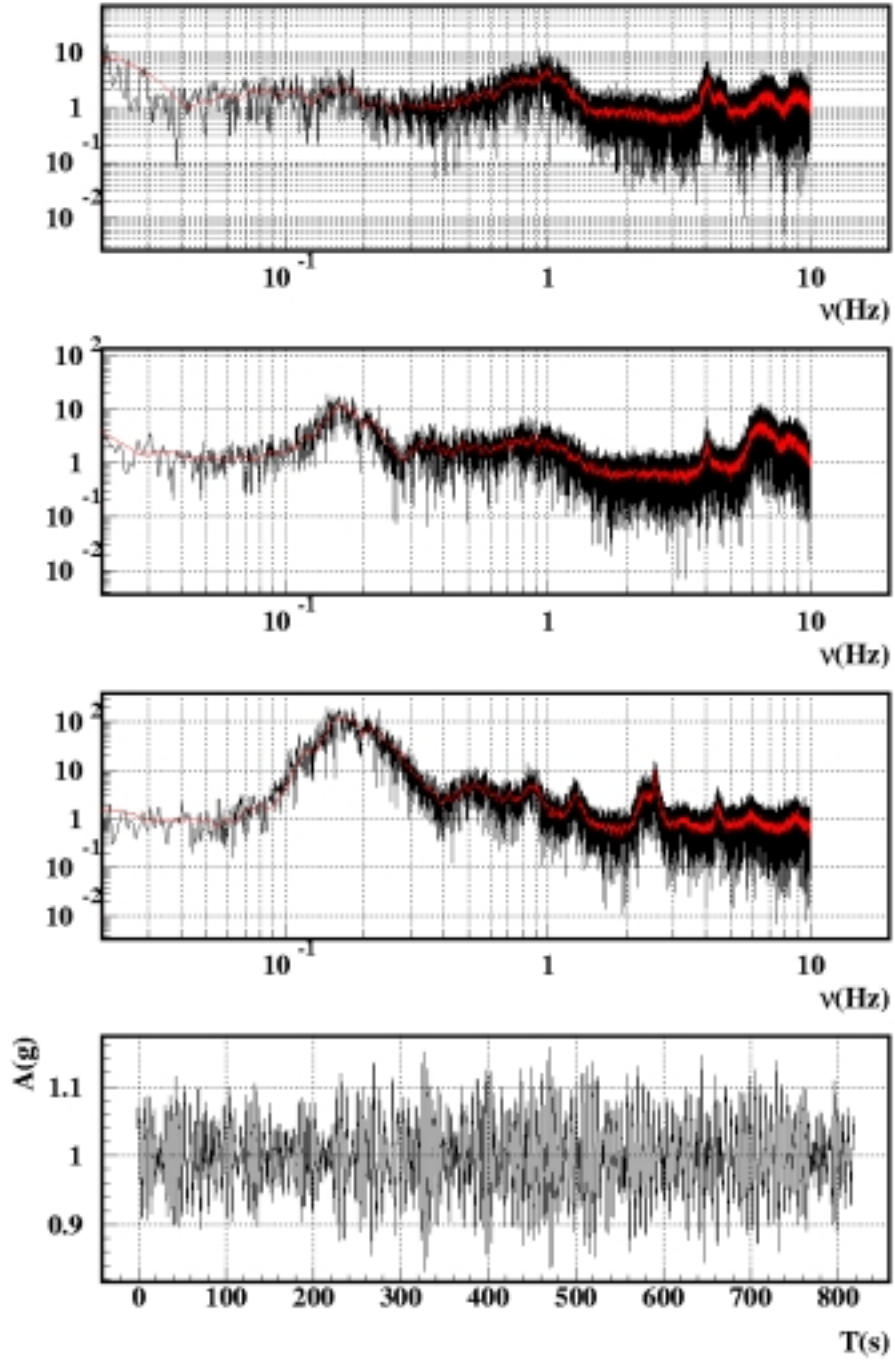


Figure 16: FFT of the acceleration measured when the line was suspended at 500 m from sea bed from 12:57 to 13:27. The plots have the same lay-out as in fig. 15.

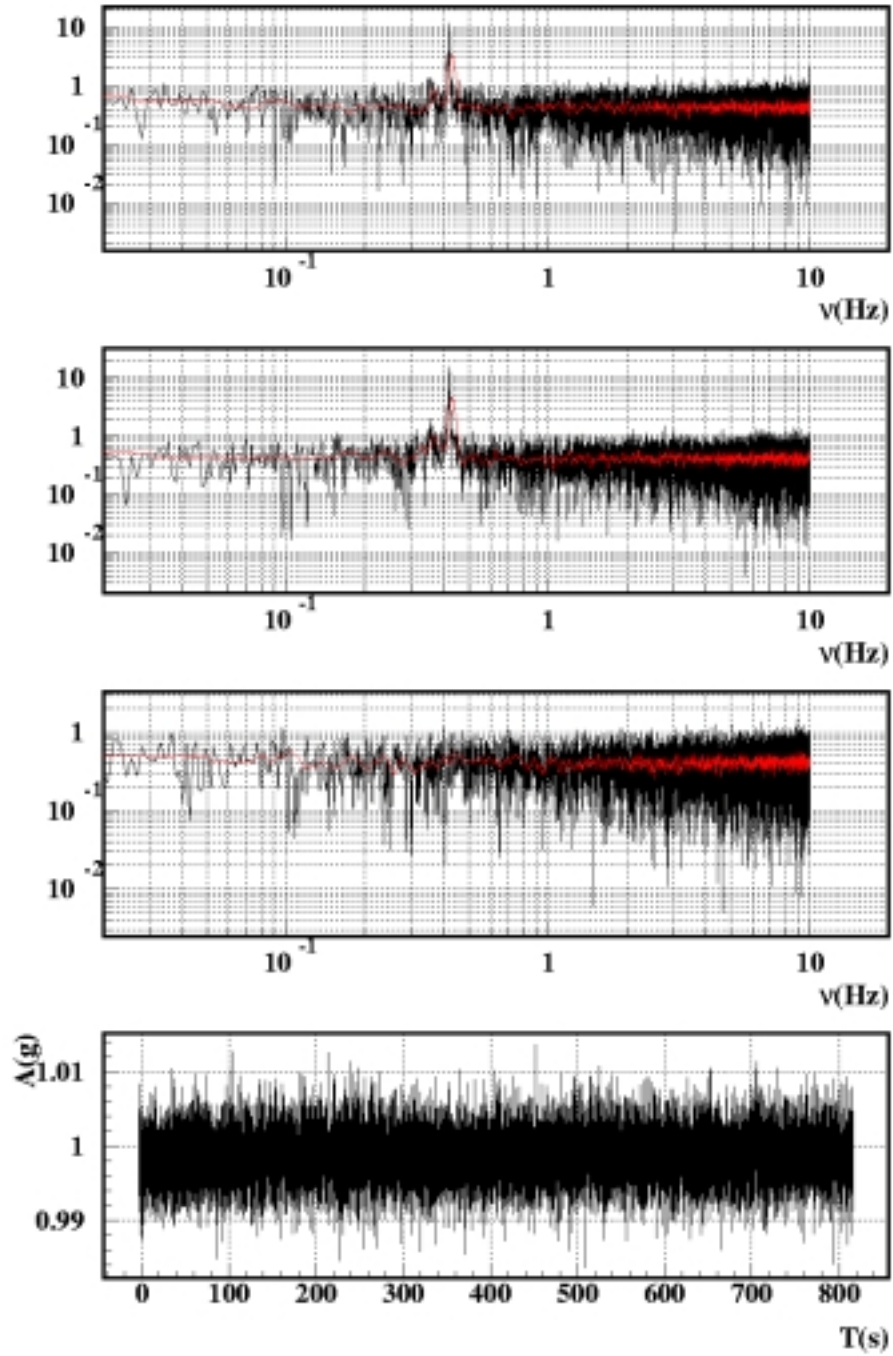


Figure 17: FFT of the acceleration measured when the line was free from 16:12 to 16:27. The plots have the same lay-out as in fig. 15.



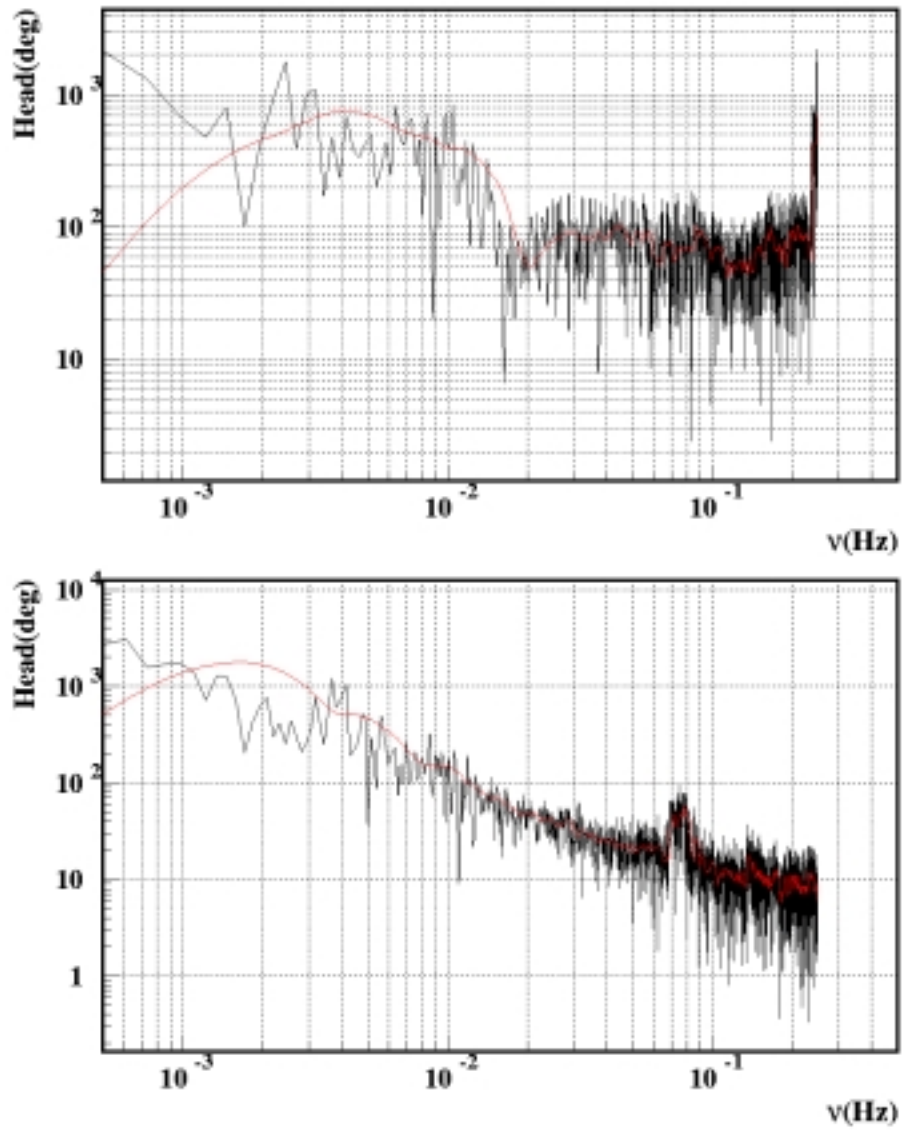


Figure 18: FFT of the head data. The top plot refers to the time interval between 12:57 to 13:27. The bottom plot refers to the interval 16:12-16:27.

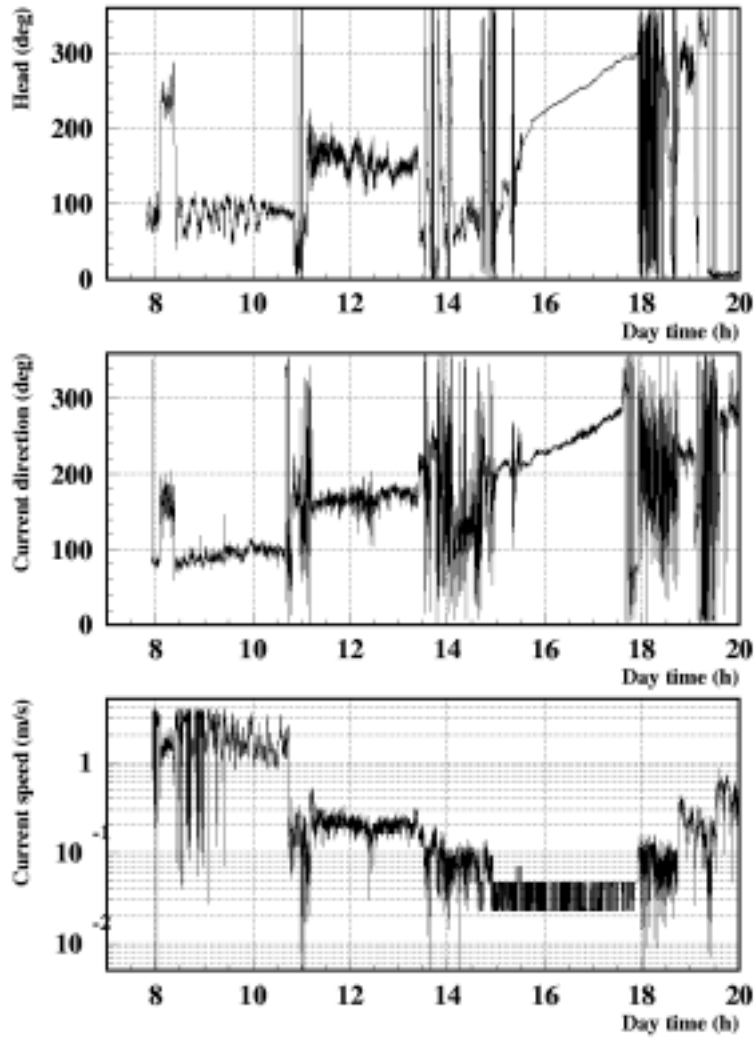


Figure 19: Comparison between the head measured by TempHuRA meter and the current direction and speed measured by the MORS VACM meter.

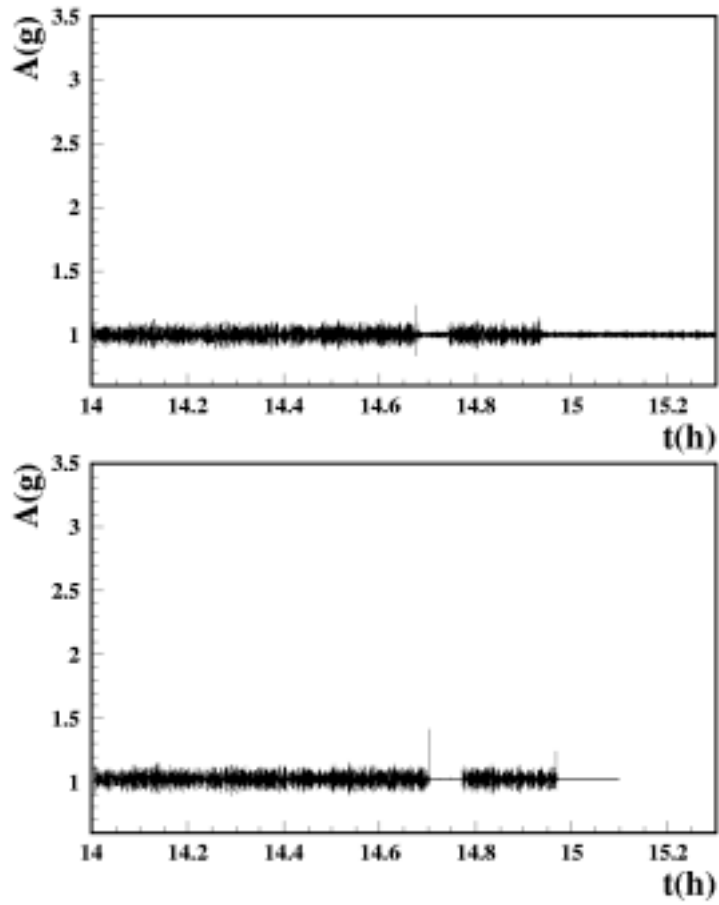


Figure 20: Comparison between the acceleration measured by the TempHuRA meter and IFREMER accelerometer.

We presented a compact stand-alone apparatus, the TempHuRA meter, able to measure and store triaxial acceleration, rotation angles, temperature and humidity with long lifetime. Tests and calibrations performed in laboratory demonstrated the reliability and the good performances of the entire apparatus. The TempHuRA meter was mounted on the ANTARES test line deployed in deep sea water in December 2001. The data collected during the 12 hours deployment test shown that the free line behavior is quite stable (no major rotation and acceleration were detected) while periodic oscillations and strong stress are induced when the line is on-board or when it is connected to the boat trough the deep sea cable. A detailed analysis of this data allowed to extract important parameters (as maximum acceleration, rotation speed, release velocity) necessary to characterize the mechanical behavior of the line during the deployment and useful to optimize the final line design.

## References

- [1] V. S. Berezinskii *et al.* ‘Astrophysics of cosmic rays’, North-Holland 1990.
- [2] V.A. Balkanov *et al.* (BAIKAL collaboration) ‘The BAIKAL neutrino project: Status report’, *Nucl. Phys. Proc. Suppl.* **91** (2000) 438
- [3] G.C. Hill (AMANDA Collaboration), ‘Results from AMANDA’, arXiv:astro-ph/0106064.
- [4] E. Carmona (ANTARES Collaboration), ‘Status Report Of The Antares Neutrino Telescope’, *Nucl. Phys. Proc. Suppl.* **95** (2001) 161.
- [5] P.K. Grieder (NESTOR Collaboration), ‘Nestor Neutrino Telescope Status Report’, *Nucl. Phys. Proc. Suppl.* **97** (2001) 105.
- [6] C.N. De Marzo (NEMO Collaboration), ‘The km<sup>3</sup> Mediterranean Neutrino Observatory - The Nemo.Rd Project’, *Nucl. Phys. Proc. Suppl.* **100** (2001) 344.
- [7] ANTARES Collaboration, *ANTARES Technical Design Report*, Version 0.3 April 2001
- [8] V. Bertin, P. Keller, ‘Qualification Tests on TCM2-20 card fro PNI’ Antares-Internal Note 3 INS 02 01 B
- [9] Antares- Internal note;  
[http://antares.in2p3.fr/internal/testlog/Instrumentation/Tiltcompass/Calib\\_BSS\\_nov01](http://antares.in2p3.fr/internal/testlog/Instrumentation/Tiltcompass/Calib_BSS_nov01)

[10] December 2001 Deployment test:

*[http://antares.in2p3.fr/users/billault/internal/sea\\_ops/castor011201/castor\\_011201.htm](http://antares.in2p3.fr/users/billault/internal/sea_ops/castor011201/castor_011201.htm)*

[11] December 2001 Deployment test:

*[http://antares.in2p3.fr/users/billault/internal/sea\\_ops/castor011201/castout.txt](http://antares.in2p3.fr/users/billault/internal/sea_ops/castor011201/castout.txt)*

[12] G. Damy, private communication.